JCTC Journal of Chemical Theory and Computation

ARTICLE

pubs.acs.org/JCTC

SHARC: *ab Initio* Molecular Dynamics with Surface Hopping in the Adiabatic Representation Including Arbitrary Couplings

Martin Richter,[†] Philipp Marquetand,[*,†] Jesús González-Vázquez,[*,†,§] Ignacio Sola,[‡] and Leticia González[†]

[†]Institut für Physikalische Chemie, Friedrich-Schiller-Universität Jena, Helmholtzweg 4, 07743 Jena, Germany

[‡]Departamento de Química Física I, Universidad Complutense, 28040 Madrid, Spain

ABSTRACT: We present a semiclassical surface-hopping method which is able to treat arbitrary couplings in molecular systems including all degrees of freedom. A reformulation of the standard surface-hopping scheme in terms of a unitary transformation matrix allows for the description of interactions like spin−orbit coupling or transitions induced by laser fields. The accuracy of our method is demonstrated in two systems. The first one, consisting of two model electronic states, validates the semiclassical approach in the presence of an electric field. In the second one, the dynamics in the IBr molecule in the presence of spin−orbit coupling after laser excitation is investigated. Due to an avoided crossing that originates from spin−orbit coupling, IBr dissociates into two channels: I + Br($^2P_{3/2}$) and I + Br*($^2P_{1/2}$). In both systems, the obtained results are in very good agreement with those calculated from exact quantum dynamical simulations.

1. INTRODUCTION

The ultimate goal of chemistry is to precisely steer chemical reactions. However, to improve the state-of-the-art control, an understanding of molecular and atomic processes including all kinds of couplings and interactions is crucial. These two points, understanding and control of chemical processes, become increasingly challenging when looking at complex systems of growing size. Experiment and theory have to work hand in hand as, e.g., spectra become very complicated and the use of exact equations is not feasible anymore. Focusing on the theoretical part, an exact description of the coupled motion of nuclei and electrons is offered by the time-dependent Schrödinger equation, but it can be solved only for the simplest systems.[1] To study bigger systems, different approximations have been developed and implemented, leading to methods like, e.g., the multiconfigurational time-dependent Hartree method (MCTDH),[2−4] multiple spawning,[5,6] or similar techniques.[7−15] An alternative is to use *ab initio* molecular dynamics (MD), where the electronic structure is treated quantum mechanically and the nuclear motion is subject to classical mechanics.[16,17] Such a classical nuclear trajectory can only be subject to one electronic potential at a time. However, several potentials are often necessary to provide a correct description of the system's dynamics. The Tully's fewest switches algorithm of surface hopping (SH) method[18,19] is one of the most prominent solutions to this predicament.

SH was initially developed to account for nonadiabatic couplings between different states. Yet, couplings like those induced by electric fields or spin−orbit couplings (SOC) are also relevant to the treatment of light-induced processes. Especially the description of the interaction between light and matter is essential for simulating many spectroscopic experiments. Moreover, the whole field of quantum control is built on these foundations.[20−29] SOC also plays a major role in modern photochemistry. Processes like intersystem crossing or phosphorescence, i.e., transitions between triplet and singlet states, determine the outcome of photochemical reactions.[30,31] Major effects are expected in molecules including heavy atoms. More unexpectedly, they also strongly affect the photochemisty of organic or biomolecules such as DNA, see, e.g., ref 32.

Despite the importance of these couplings, only few methods exist which incorporate one or the other of those effects in MD.[33−37] To our knowledge, no MD method is able so far to handle all of the couplings simultaneously in a straightforward way. In this paper, we present a method which, derived from the original SH scheme, allows one to treat arbitrary couplings without introducing any further approximations. In this way, a semiclassical description of the coupled electronic and nuclear motion with laser interaction in complex molecular systems including all degrees of freedom is feasible. In principle, not only SOC or laser interactions can be included but all imaginable couplings can be straightforwardly considered by our surface-hopping-in-adiabatic-representation-including-arbitrary-couplings (SHARC) method. The SH probabilities are calculated in terms of a unitary transformation matrix which diagonalizes the matrix containing the considered electronic potentials and all possible couplings at once.

In order to demonstrate the effectiveness of SHARC, two test systems are chosen in this paper: two coupled harmonic oscillators first and then the excited-state dissociation in the IBr molecule. IBr exhibits strong SOC, leading to an avoided crossing between two excited states, the $1^3\Pi_{0+}$ and the $1^3\Sigma^-_{0+}$ states, see ref 38 and references therein. These two states are responsible for the product channels resulting in I + Br and I + Br*, respectively.[39] The asterisk denotes the $^2P_{1/2}$ excited spin-state of the dissociating Br atom, while the ground state has the configuration $^2P_{3/2}$. The outcome from SHARC simulations is compared with results from exact quantum-dynamical calculations.

Received: January 28, 2011
Published: March 29, 2011

The methodology and the theoretical description are presented in section 2. The numerical results are contained in section 3, and a summary is given in section 4.

2. METHODOLOGY

The time evolution of the system is followed using a mix of quantum and classical dynamics, where the electrons are treated quantum mechanically and the nuclei classically. The interaction between the quantum and the classical part is described in two ways. On the one hand, the nuclei follow the quantum potential created by the electrons using classical trajectories. These trajectories are defined by the position $\vec{R}(t)$ and velocity $\vec{v}(t)$ of the nuclei at every time. On the other hand, the electronic wave function depends on the electronic coordinates $(\vec{r})$ and parametrically on the nuclei coordinates. The electronic wave function is defined by $|\Psi[\vec{R}(t);\vec{r},t]\rangle$, and the potential that governs the evolution of the classical trajectory is given by the expectation value of an effective Hamiltonian $V(t) = \langle\Psi(\vec{R}(t);\vec{r},t)|\hat{H}_{\text{eff}}[\vec{R}(t),\vec{r}]|\Psi(\vec{R}(t);\vec{r},t)\rangle$. $\hat{H}_{\text{eff}}$ depends parametrically on the nuclear coordinates, and it includes the nucleus−nucleus repulsion, the electron−nucleus attraction, the electron−electron, and the electronic kinetic energy.

In quantum mechanics, the position and velocity of the nuclei cannot be simultaneously known. This uncertainty is described in our classical dynamics by considering a set of initial conditions for the trajectories. This set mimics the initial nuclear quantum probability creating a swarm of trajectories. Every single trajectory is propagated using Newton's equations with the Velocity Verlet algorithm.[40,41] In this algorithm, the time evolution of the nuclear coordinates $\vec{R}(t)$ is driven by the gradient of the potential at time t:

$$\vec{R}(t+\Delta t) = \vec{R}(t) + \vec{v}(t)\Delta t + \frac{1}{2M}\nabla_{\vec{R}} V(t)\,\Delta t^2 \qquad (1)$$

where M represents the mass of the nuclei. Finally, the velocity is propagated using the gradient of the potential at times t and $t + \Delta t$:

$$\vec{v}(t+\Delta t) = \vec{v}(t) + \frac{1}{2M}\nabla_{\vec{R}} V(t)\,\Delta t + \frac{1}{2M}\nabla_{\vec{R}} V(t+\Delta t)\Delta t \qquad (2)$$

The definition of the potential is given by the time evolution of the electronic wavepacket following the time-dependent Schrödinger equation:

$$i\hbar\frac{\partial|\Psi[\vec{R}(t);\vec{r},t]\rangle}{\partial t} = \hat{H}_{\text{eff}}[\vec{R}(t);\vec{r}]|\Psi[\vec{R}(t);\vec{r},t]\rangle \qquad (3)$$

In order to solve this equation, we expand the wavepacket as a linear combination of basis functions at different $\vec{R}(t)$:

$$|\Psi[\vec{R}(t);\vec{r},t]\rangle = \sum_\alpha c_\alpha(t)|\phi_\alpha[\vec{R}(t);\vec{r}]\rangle \qquad (4)$$

Using this formalism, the time evolution of the coefficients is described by

$$\frac{\partial c_\beta(t)}{\partial t} = -\sum_\alpha\left\{\frac{i}{\hbar}H_{\beta\alpha}[\vec{R}(t)] + K_{\beta\alpha}[\vec{R}(t)]\right\}c_\alpha(t) \qquad (5)$$

where $H_{\beta\alpha}[\vec{R}(t)] = \langle\phi_\beta[\vec{R}(t);\vec{r}]|\hat{H}_{\text{eff}}[\vec{R}(t);\vec{r}]|\phi_\alpha[\vec{R}(t);\vec{r}]\rangle$ represents the diabatic Hamiltonian whose diagonal elements are the different potentials and the off-diagonal elements are the diabatic couplings. The second term,

$$K_{\beta\alpha}[\vec{R}(t)] = \langle\phi_\beta[\vec{R}(t);\vec{r}]|\partial/\partial t|\phi_\alpha[\vec{R}(t);\vec{r}]\rangle \qquad (6)$$

evaluates the change of the electronic basis functions with time, which is equivalent to the variation of the basis with the nuclear coordinates times the velocity:

$$\begin{aligned}K_{\beta\alpha}[\vec{R}(t)] &= \langle\phi_\beta[\vec{R}(t);\vec{r}]|\partial/\partial t|\phi_\alpha[\vec{R}(t);\vec{r}]\rangle \\ &= \langle\phi_\beta[\vec{R}(t);\vec{r}]|d/d\vec{R}(t)|\phi_\alpha[\vec{R}(t);\vec{r}]\rangle\,\vec{v}(t)\end{aligned} \qquad (7)$$

This equation is solved using a simple Runge−Kutta algorithm of fourth order.

The definition of the basis functions is very important in this methodology. The most common way to define the basis functions of the electronic wavepacket is using the eigenfunctions of the time-independent Schrödinger equation for every $\vec{R}(t)$. In this way, the effective Hamiltonian is the adiabatic energy of the different electronic states $H_{\beta\alpha}[\vec{R}(t)] = V_\alpha[\vec{R}(t)]\delta_{\beta\alpha}$, while $K_{\beta\alpha}[\vec{R}(t)]$ is related to the nonadiabatic coupling elements that break the Born−Oppenheimer approximation. However, the trajectories cannot be spread over several electronic states, and hence, it is necessary to assign the electronic state that governs the trajectory dynamics at each time. In this work, we employ the SH method proposed by Tully,[18] where the classical trajectory is propagated in a single potential β. In order to take into account nonadiabatic effects, the trajectory can jump from one to another state. The probability for such a hop is calculated using the time-dependent coefficients of the electronic wave function:

$$P_{\beta\alpha} = \frac{2\mathscr{R}\left\{c_\beta^*(t)\,c_\alpha(t)\left[\frac{i}{\hbar}H_{\beta\alpha}[\vec{R}(t)] + K_{\beta\alpha}[\vec{R}(t)]\right]\right\}}{c_\beta^*(t)\,c_\beta(t)}\Delta t \qquad (8)$$

This methodology is widely used to simulate relaxation dynamics via conical intersections where large kinetic couplings are localized around the degeneration points.[42,43] In this work, we extend SH to the situation where SOCs and/or the interaction with an electric field must be included in the dynamical simulation. These two terms are typically evaluated in the diabatic representation, and thus they are included in the potential part of the Hamiltonian, introducing a new $H^d[\vec{R}(t)]$ matrix with elements (where the index d indicates that additional nondiagonal terms are included):

$$H^d_{\beta\alpha}[\vec{R}(t),t] = H_{\beta\alpha}[\vec{R}(t)] - \vec{\mu}_{\beta\alpha}[\vec{R}(t)]\,\vec{\mathscr{E}}(t) + \hat{H}^{\text{SO}}_{\beta\alpha}[\vec{R}(t)] \qquad (9)$$

In this equation, $\vec{\mu}_{\beta\alpha}[\vec{R}(t)]$ and $\hat{H}^{\text{SO}}_{\beta\alpha}[\vec{R}(t)]$ are the dipole moment and the relativistic spin−orbit coupling between the states β and α, respectively.

In contrast to the relaxation dynamics via conical intersections (nonadiabatic couplings), this new Hamiltonian contains off-diagonal elements which may be extremely extended in space, making the solution of the corresponding equations not an easy task. As such off-diagonal elements are responsible for the jumps, spatially delocalized couplings might induce jumps at all geometries contradicting the idea of the fewest switches criterion. Especially SOCs are usually very much extended in space, see,

e.g., ref 38. In SHARC, this problem is solved by translating the coupling elements to the $K[\vec{R}(t)]$ matrix. In this adiabatic (index a) approach, the $H^d[\vec{R}(t),t]$ matrix is diagonalized, and afterwards, the $K[\vec{R}(t)]$ matrix is recalculated, leading to localized couplings in geometries where the electronic states are (nearly) degenerated.

The idea exploited here is the substitution of the basis set of electronic wave functions $|\phi^d[\vec{R}(t);r]\rangle$ for a linear combination:

$$|\phi^a_\beta[\vec{R}(t);\ \vec{r},t]\rangle = \sum_\alpha U_{\beta\alpha}[\vec{R}(t),t]|\phi^d_\alpha[\vec{R}(t);\ \vec{r}]\rangle \qquad (10)$$

where $U[\vec{R}(t),t]$ is the unitary matrix that diagonalizes the Hamiltonian $H^d[\vec{R}(t),t]$ matrix at every time t. In this new basis, the elements of the $H^a[\vec{R}(t),t]$ matrix are defined as

$$H^a_{\beta\alpha}[\vec{R}(t),t] = V^a_\alpha[\vec{R}(t),t]\delta_{\beta\alpha} \qquad (11)$$

where $V^a_\alpha[\vec{R}(t),t]$ are the diagonal elements of $H^a[\vec{R}(t),t]$. The nonadiabatic coupling comes from the derivative of the $|\phi^a[\vec{R}(t);\vec{r},t]\rangle$:

$$K^a_{\beta\alpha}[\vec{R}(t),t] = \left\langle \phi^{a*}_\beta[\vec{R}(t);\ \vec{r},t]\left|\frac{\partial}{\partial t}\right|\phi^a_\alpha[\vec{R}(t);\ \vec{r},t]\right\rangle$$

$$= K^\phi_{\beta\alpha}[\vec{R}(t),t] + K^U_{\beta\alpha}[\vec{R}(t),t] \qquad (12)$$

where $K^\phi_{\beta\alpha}[\vec{R}(t),t]$ and $K^U_{\beta\alpha}[\vec{R}(t),t]$ are the nonadiabatic terms in the original basis $|\phi^d[\vec{R}(t);\vec{r}]\rangle$ and those induced via the rotation matrix $U[\vec{R}(t),t]$.

The first term $K^\phi[\vec{R}(t),t]$ is just the rotation of the original nonadiabatic term to the new basis:

$$K^\phi_{\beta\alpha}[\vec{R}(t),t]$$
$$= \sum_{\lambda\gamma} U^*_{\lambda\beta}[\vec{R}(t),t]K_{\lambda\gamma}[\vec{R}(t)]U_{\gamma\alpha}[\vec{R}(t),t]$$
$$= \vec{v}(t)\sum_{\lambda\gamma} U^*_{\lambda\beta}[\vec{R}(t),t]\langle\phi^d_\gamma[\vec{R}(t);\ \vec{r}]|\nabla_{\vec{R}}|\phi^d_\gamma[\vec{R}(t);\ \vec{r}]\rangle U_{\gamma\alpha}[\vec{R}(t),t] \qquad (13)$$

and the other component comes from the variation of the rotation matrix:

$$K^U_{\beta\alpha}[\vec{R}(t),t] = \sum_\lambda U^*_{\lambda\beta}[\vec{R}(t),t]\frac{\partial}{\partial t}U_{\lambda\alpha}[\vec{R}(t),t]$$
$$= \vec{v}(t)\sum_\lambda U^*_{\lambda\beta}[\vec{R}(t),t]\nabla_{\vec{R}}U_{\lambda\alpha}[\vec{R}(t),t] \qquad (14)$$

To obtain the new potentials $V^a[\vec{R}(t),t]$ and the nonadiabatic coupling elements $K^a[\vec{R}(t),t]$, the matrix $H^d[\vec{R}(t),t]$ is diagonalized at distances $\vec{R}(t)$,$\vec{R}(t)+\Delta\vec{R}$, and $\vec{R}(t)-\Delta\vec{R}$. In this fashion, the gradient of the potential and the gradient of the $U[\vec{R}(t),t]$ matrix are evaluated. These new matrices are used in eqs 5 and 8 to calculate the nonadiabatic dynamics.

In the original SH method, the velocity of a trajectory is adjusted after a jump in order to conserve energy. This, however, is not reasonable for laser transitions. Therefore, we do not adjust the kinetic energy as long as the resonance condition is fulfilled, i.e., as long as the potential energy difference of the involved states lies within the laser bandwidth.

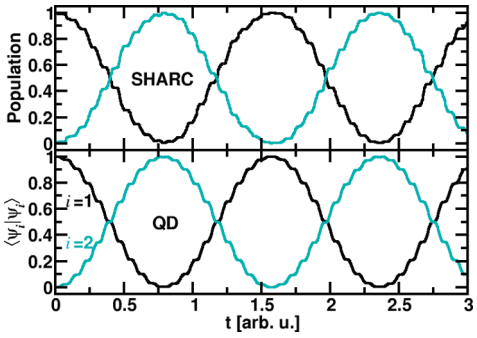

Figure 1. Comparison of the population dynamics calculated via SHARC (upper panel) or QD (lower panel) in a system consisting of two harmonic oscillators. Rabi oscillations of the populations in the ground state (i = 1; black) and the excited state (i = 2; turquoise) are clearly visible in both cases.

3. NUMERICAL RESULTS

In what follows, two model systems are investigated. First, we consider the modeling of Rabi oscillations between two harmonic oscillators using SHARC. Second, the branching ratio of excited-state dissociation products of IBr is examined. The motivation behind these rather simple models is to be able to compare the results of SHARC with those from exact quantum dynamics (QD). For the quantum part, the time-dependent Schrödinger equation is solved employing the split-operator method.[44] Solutions of the stationary Schrödinger equation are obtained by imaginary time propagation.[45] From these solutions, Wigner distributions are obtained and used to establish the initial conditions in the MD simulations.

As a first model system, we consider two vertically displaced one-dimensional harmonic oscillators defined by

$$V_1(R) = \frac{1}{2}kR^2 \qquad (15)$$

$$V_2(R) = \frac{1}{2}kR^2 + D_{12} \qquad (16)$$

where k and D_{12} are 1 and 40 in dimensionless units. The reduced mass is taken to be 1, and the transition dipole moment between the states is μ_{12} = 1. The two potentials are coupled by a *cw* field:

$$E(t) = A\sin(\omega t) \qquad (17)$$

where A = 4 and $\omega = D_{12}$ to induce a resonant transition.

For both MD and QD calculations, a time step of 0.002 was employed. A set of 500 trajectories was used in the MD simulations, although the results are converged already after 100 trajectories.

The time-dependent populations calculated from SHARC and QD are shown in Figure 1. Rabi oscillations are clearly visible in both cases. More precisely, the curves from SHARC and QD show exactly the same behavior. Therefore, the SHARC approach is capable of describing laser-induced processes. However, this approach is not limited to dipole-type couplings but can treat simultaneously any other kind of coupling, as will be shown in the next example.

As a second model system, we look at the IBr molecule and its excited-state dissociation. In order to compare our MD results directly with those of QD simulations, we restrict ourselves to the

dx.doi.org/10.1021/ct1007394 |J. Chem. Theory Comput. 2011, 7, 1253–1258

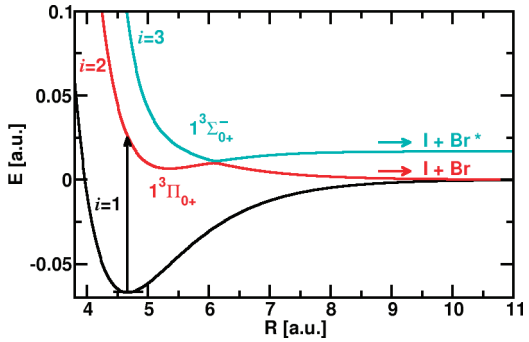

Figure 2. Potential energy curves of the IBr molecule and excitation scheme. IBr molecules initially in the electronic ground state (black) are excited to the $1^3\Pi_{0+}$ excited electronic state (red) and can undergo dissociation into two different channels due to an avoided crossing introduced by SOC with the $1^3\Sigma^-_{0+}$ excited state (turquoise).

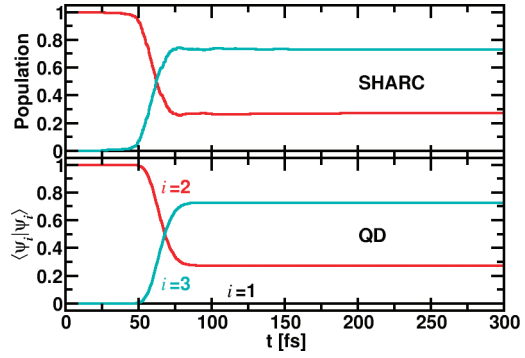

Figure 3. Population dynamics in the excited states of IBr after excitation with a δ pulse computed with the SHARC algorithm (upper panel) and QD (lower panel). After around 65 fs, an avoided crossing is passed, which gives rise to a branching ratio $Q = 72\%$ of the products in the different dissociation channels (I + Br in state $i = 2$ and I + Br* in state $i = 3$) with both simulation types. The ground state ($i = 1$; black) is not populated.

model potentials from ref 46. Note that even if here we limit ourselves to analytical potentials in order to benchmark SHARC in the presence of SOC and laser interactions, more complex systems can be tackled easily using "on the fly" electronic structure calculations.

IBr is a good candidate since it is a diatomic, which can be treated conveniently with QD, and it exhibits large SOC. Due to the latter coupling, the $1^3\Pi_{0+}$ and the $1^3\Sigma^-_{0+}$ state potentials show an avoided crossing at around $R = 6.1$ au = 3.2 Å, see Figure 2, which otherwise would not exist since the two states are of different symmetry. Moreover, it is only because of SOC that the excited-state dissociation channels differ in energy, see ref 38. In the present model, the dissociation products are I + Br or I + Br*, respectively.

To test whether the SOC is treated correctly within SHARC, we excite the ground state population first with a δ pulse to the $1^3\Pi_{0+}$ state and look at the population dynamics. In both the MD and QD simulations, the propagation time step is 0.02 fs. Again, 500 trajectories are considered in the MD case. It is gratifying to see (Figure 3) that the results of both calculations are in perfect agreement. The branching ratio of the dissociation products, defined as $Q = ([I + Br^*])/([I + Br] + [I + Br^*])$, is equal to 72% in both cases.

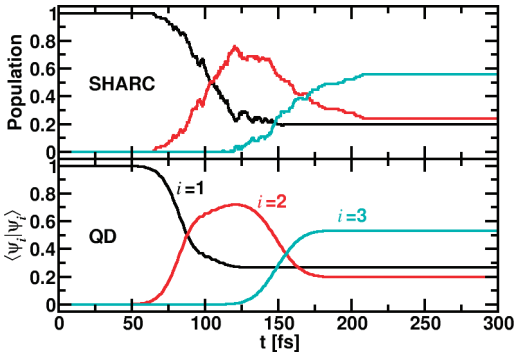

Figure 4. Population dynamics in IBr after excitation with a 50 fs fwhm pulse computed with the SHARC algorithm (upper panel) and QD (lower panel). The population in the ground state ($i = 1$) is depicted in black, the first excited state ($i = 2$) in red, and the second excited state ($i = 3$) in turquoise. The excitation yield from the SHARC simulation ($Y = 80\%$) is in good agreement with the one from the QD calculation ($Y = 73\%$). Also, the branching ratio of excited state products is in very good agreement ($Q = 70\%$ from SHARC vs $Q = 73\%$ from QD).

As a second scenario, we treat the spin−orbit and strong laser-field induced couplings at the same time in the MD simulation. The laser pulse has a finite duration, and it is of Gaussian shape with the electric field's fwhm (full width at half-maximum) of 50 fs centered at $t = 100$ fs and a field strength of 0.00534 au (corresponding to an intensity of 1 TW/cm^2). The wavelength for the laser excitation from the electronic ground state is set to 493 nm to satisfy the resonance condition with the $1^3\Pi_{0+}$ electronic state. As in the previous simulation, we use a time step of 0.02 fs and 500 trajectories in SHARC.

Figure 4 shows the time-dependent populations calculated via SHARC (upper panel) and via QD (lower panel). Very good agreement is also found between the two simulations. First, we look at the excitation yield Y. After the laser pulse is over, $Y = 80\%$ of the population has been excited according to SHARC and $Y = 73\%$ according to QD. Second, we compare the resulting branching ratios; this is calculated as $Q = 70\%$ from SHARC and $Q = 73\%$ from QD. Although we used 500 trajectories to get this number in the MD case, a branching ratio of $Q = 69\%$ is already obtained after only 100 trajectories. It is very encouraging that the deviations are very small, especially taking into account that there is no coherent interaction possible between the individual trajectories. Even the momentum distributions in the respective states are almost identical for the different algorithms, see Figure 5. This latter property is of great importance in numerous applications, e.g., the simulation of velocity map imaging.[47] In Figure 5, the momentum distribution of the ground state is the fraction centered around $p = 0$ au. After the laser excitation, when the $1^3\Pi_{0+}$ state is populated, there is a quick gain of momentum in this state. The passing through the avoided crossing is visible in the form of a splitting of the momentum distribution at later times (ca. 160 fs). The momentum distribution clearly indicates that the largest amount of trajectories (SHARC) or the wavepacket (QD) changes the adiabatic state to yield I + Br*; see that due to the climbing of the potential slope, the momentum diminishes. The rest of the excited state momentum distribution stems from the state resulting in I + Br, where additional momentum is collected during the dissociation.

Albeit rather simple at first sight, IBr turns out to be quite an extreme test case. It possesses an intermediate SOC strength

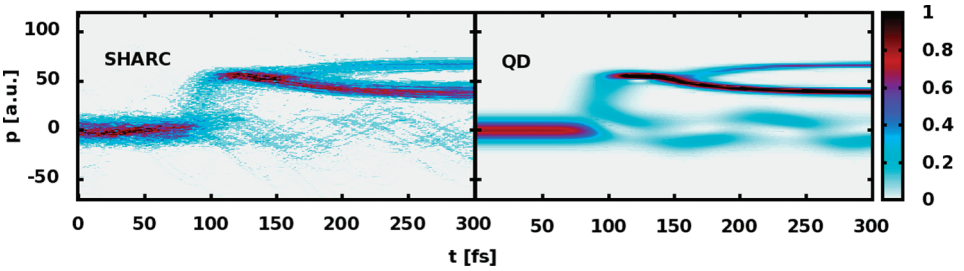

Figure 5. Time-dependent momentum probability distribution as calculated from SHARC (left panel) and QD (right panel).

such that neither the pure adiabatic nor the pure diabatic picture completely describe its dynamics.[48] In a two-level system, this is indeed the worst-case scenario. Moreover, the excited state potentials are extremely steep in the Franck−Condon region. As a consequence, even a narrow distribution of initial conditions in the ground state will result in the most different momenta in the excited state at the time the avoided crossing is reached. Finally, the ground state potential is very anharmonic due to the SOC. Despite these hurdles, SHARC is able to correctly describe the complete dynamics influenced by laser interactions and SOC.

4. CONCLUSION

To summarize, here, we present a new surface-hopping-in-adiabatic-representation-including-arbitrary-couplings (SHARC) algorithm, where the surface hopping probabilities are calculated in terms of a unitary transformation matrix. Within this semiclassical scheme, a matrix containing the considered electronic potentials and all possible couplings is diagonalized at once. In this way, we are able to treat all kinds of couplings in molecular systems including all degrees of freedom on the same footing. While the motion of the nuclei is treated classically, the potentials entering into the propagation can stem from simple analytical functions (as it was exemplarily done here to compare explicitly with exact quantum dynamics), complex parametrized force fields, or semiempirical or state-of-the-art *ab initio* methods.

We have therefore shown that, besides nonadiabatic couplings, field-induced transitions to triplet states can henceforth be treated within molecular dynamics. In this way, the often neglected influence of triplet states in the dynamics of most different molecules can be investigated using semiclassical simulations. The treatment of large systems, which may even include molecules in solution, is straightforward by computing the potential energies "on the fly".

AUTHOR INFORMATION

Corresponding Author

*E-mail: p.marquetand@uni-jena.de (P.M.); jgv@tchiko.quim.ucm.es (J.G.-V.).

Present Addresses

[§]Departamento de Química Física I, Universidad Complutense, 28040 Madrid, Spain.

ACKNOWLEDGMENT

This work has been supported by the Deutsche Forschungsgemeinschaft (DFG) within the project GO 1059/6-1, the German Federal Ministry of Education and Research within the research initiative PhoNa, the Dirección General de Investigación of Spain under Project No. CTQ2008-06760, the Friedrich-Schiller-Universität Jena, and a Juan de la Cierva contract. Generous allocation of computer time at the Computer center of the Friedrich-Schiller-Universität is gratefully acknowledged.

REFERENCES

(1) Tannor, D. *Introduction to Quantum Mechanics: A Time-Dependent Perspective*; University Science Books: Sausalito, CA, 2006.
(2) Beck, M. H.; Jäckle, A.; Worth, G. A.; Meyer, H. D. *Phys. Rep* **2000**, *324*, 1–105.
(3) Bowman, J. M.; Carrington, T.; Meyer, H. *Mol. Phys.* **2008**, *106*, 2145–2182.
(4) Worth, G. A.; Meyer, H. D.; Köppel, H.; Cederbaum, L. S.; Burghardt, I. *Int. Rev. Phys. Chem.* **2008**, *27*, 569–606.
(5) Virshup, A. M.; Punwong, C.; Pogorelov, T. V.; Lindquist, B. A.; Ko, C.; Martínez, T. J. *J.Phys. Chem. B* **2009**, *113*, 3280–3291.
(6) Levine, B. G.; Coe, J. D.; Virshup, A. M.; Martínez, T. *J. Chem. Phys.* **2008**, *347*, 3–16.
(7) Worth, G. A.; Robb, M. A.; Burghardt, I. *Faraday Discuss* **2004**, *127*, 307–323.
(8) Rassolov, V. A.; Garashchuk, S. *Phys. Rev. A* **2005**, *71*, 032511.
(9) Li, J.; Woywod, C.; Vallet, V.; Meier, C. *J. Chem. Phys.* **2006**, *124*, 184105.
(10) Spezia, R.; Burghardt, I.; Hynes, J. T. *Mol. Phys.* **2006**, *104*, 903–914.
(11) Lasorne, B.; Robb, M. A.; Worth, G. A. *Phys. Chem. Chem. Phys.* **2007**, *9*, 3210–3227.
(12) Shalashilin, D. V.; Child, M. S.; Kirrander, A. *Chem. Phys.* **2008**, *347*, 257–262.
(13) Yonehara, T.; Takahashi, S.; Takatsuka, K. *J. Chem. Phys.* **2009**, *130*, 214113.
(14) Yonehara, T.; Takatsuka, K. *J. Chem. Phys.* **2010**, *132*, 244102.
(15) Granucci, G.; Persico, M.; Zoccante, A. *J. Chem. Phys.* **2010**, *133*, 134111.
(16) Marx, D., Hutter, J. *Ab Initio Molecular Dynamics: Basic Theory and Advanced Methods*; Cambridge University Press: Cambridge, U. K., 2009.
(17) Doltsinis, N.; Marx, D. *J. Theory Comput. Chem.* **2002**, *1*, 319–349.
(18) Tully, J. C. J. *Chem. Phys.* **1990**, *93*, 1061–1071.
(19) Doltsinis, N. In *Computational Nanoscience: Do It Yourself!*; Grotendorst, J., Ed.; John von Neumann-Institut für Computing: Jülich, Germany, 2006; pp 389−409.
(20) Brumer, P.; Shapiro, M. *Annu. Rev. Phys. Chem.* **1992**, *43*, 257–282.
(21) Gordon, R. J.; Rice, S. A. *Annu. Rev. Phys. Chem.* **1997**, *48*, 601–641.
(22) Rice, S. A. *Adv. Chem. Phys.* **1997**, *101*, 213–283.
(23) Tannor, D. J.; Kosloff, R.; Bartana, A. *Faraday Discuss.* **1999**, *113*, 365–383.
(24) Shapiro, M.; Brumer, P. *Rep. Prog. Phys.* **2003**, *66*, 859–942.
(25) Rice, S. A.; Zhao, M. *Optical Control of Molecular Dynamics*; Wiley: New York, 2000.

(26) Shapiro, M.; Brumer, P. *Principles of Quantum Control of Molecular Processes*; Wiley: New York, 2003.
(27) Brixner, T.; Damrauer, N. H.; Gerber, G. *Adv. At. Mol. Opt. Phys.* **2001**, *46*, 1–54.
(28) Nuernberger, P.; Vogt, G.; Brixner, T.; Gerber, G. *Phys. Chem. Chem. Phys.* **2007**, *9*, 2470–2497.
(29) Engel, V.; Meier, C.; Tannor, D. J. *Adv. Chem. Phys.* **2009**, *141*, 29–101.
(30) Reiher, M.; Wolf, A. *Relativistic Quantum Chemistry*; Wiley-VCH: Weinheim, Germany, 2009.
(31) Fedorov, D. G.; Koseki, S.; Schmidt, M. W.; Gordon, M. S. *Int. Rev. Phys. Chem.* **2003**, *22*, 551–592.
(32) González-Luque, R.; Climent, T.; González-Ramírez, I.; Merchán, M.; Serrano-Andrés, L. *J. Chem. Theory Comput.* **2010**, *6*, 2103–2114.
(33) Maiti, B.; Schatz, G. C.; Lendvay, G. *J. Phys. Chem. A* **2004**, *108*, 8772–8781.
(34) Yagi, K.; Takatsuka, K. *J. Chem. Phys.* **2005**, *123*, 224103.
(35) Jones, G. A.; Acocella, A.; Zerbetto, F. J. *Phys. Chem. A* **2008**, *112*, 9650–9656.
(36) Mitrić, R.; Petersen, J.; Bonačić-Koutecký, V. *Phys. Rev. A* **2009**, *79*, 053416.
(37) Tavernelli, I.; Curchod, B. F. E.; Rothlisberger, U. *Phys. Rev. A* **2010**, *81*, 052508.
(38) Patchkovskii, S. *Phys. Chem. Chem. Phys.* **2006**, *8*, 926–940.
(39) Sussman, B. J.; Townsend, D.; Ivanov, M. Y.; Stolow, A. *Science* **2006**, *314*, 278–281.
(40) Verlet, L. *Phys. Rev.* **1967**, *159*, 98–103.
(41) Verlet, L. *Phys. Rev.* **1968**, *165*, 201–214.
(42) Barbatti, M.; Aquino, A. J. A.; Szymczak, J. J.; Nachtigallová, D.; Hobza, P.; Lischka, H. P. *Natl. Acad. Sci. USA* **2010**, *107*, 21453 −21458.
(43) González-Vázquez, J.; González, L. *Chem. Phys. Chem.* **2010**, *11*, 3617–3624.
(44) Feit, M. D.; Fleck, J. A., Jr.; Steiger, A. *J. Comput. Phys.* **1982**, *47*, 412–433.
(45) Kosloff, R.; Tal-Ezer, H. *Chem. Phys. Lett.* **1986**, *127*, 223–230.
(46) Guo, H. *J. Chem. Phys.* **1993**, *99*, 1685–1692.
(47) Whitaker, B. *Femtosecond Chemistry*; Cambridge University Press: Cambridge, U. K., 2003; Vols. I, II.
(48) Shapiro, M.; Vrakking, M. J. J.; Stolow, A. *J. Chem. Phys.* **1999**, *110*, 2465–2473.